

Involvement of Secreted *Aspergillus fumigatus* Proteases in Disruption of the Actin Fiber Cytoskeleton and Loss of Focal Adhesion Sites in Infected A549 Lung Pneumocytes

Tanya V. Kogan,¹ Jeries Jadoun,¹ Leonid Mittelman,² Koret Hirschberg,³ and Nir Osherov¹

¹Department of Human Microbiology, ²Interdepartmental Core Facility, and ³Department of Pathology, Sackler School of Medicine, Tel Aviv University, Tel Aviv, Israel

Aspergillus fumigatus is an opportunistic pathogenic fungus that predominantly infects the respiratory system. Penetration of the lung alveolar epithelium is a key step in the infectious process. The cytoskeleton of alveolar epithelial cells forms the cellular basis for the formation of a physical barrier between the cells and their surroundings. This study focused on the distinct effects of *A. fumigatus* on the actin cytoskeleton of A549 lung pneumocytes. Of the 3 major classes of cytoskeletal fibers—actin microfilaments, microtubules, and intermediate filaments—only the actin cytoskeleton was found to undergo major structural changes in response to infection, including loss of actin stress fibers, formation of actin aggregates, disruption of focal adhesion sites, and cell blebbing. These changes could be specifically blocked in wild-type strains of *A. fumigatus* by the addition of antipain, a serine and cysteine protease inhibitor, and were not induced by an alkaline serine protease-deficient strain of *A. fumigatus*. Antipain also reduced, by ~50%, fungal-induced A549 cell detachment from the plates and reduction in viability. Our findings suggest that *A. fumigatus* breaches the alveolar epithelial cell barrier by secreting proteases that act together to disorganize the actin cytoskeleton and destroy cell attachment to the substrate by disrupting focal adhesions.

Aspergillus fumigatus is an important opportunistic pathogen in immunocompromised patients. In invasive pulmonary aspergillosis, which often is fatal, the fungus can spread from the initial site of infection in the lungs to attack various organs in the body. Mortality from this disease is high (>90% in untreated patients and 50%–70% in treated patients) [1].

A. fumigatus can bind to various types of substrates, particularly to proteins of the extracellular matrix, by means of polysaccharides and glycoproteins covering the conidial cell wall [2, 3]. Various agents secreted by the fungus into the environment during germination

also enhance initial colonization of the host's lung tissue. These agents include enzymes, such as proteases, and toxins. *A. fumigatus* secretes a variety of proteases, 3 of which have been described elsewhere: an alkaline serine protease (*ALP*) [4–6], a metalloprotease (*Mep*) [7], and an aspartic protease (*Pep*) [8]. Nevertheless, *A. fumigatus* mutant strains lacking ≥ 1 of these genes retain their virulence [9]. Although the role of secreted proteases in *A. fumigatus* infection remains unclear, it is thought that they play a role in degrading and breaching the extracellular matrix barrier in the host [9].

Lung epithelium cells constitute the main physical barrier to *A. fumigatus* infection. In vitro studies using the A549 human lung carcinoma cell line as a model have demonstrated that conidia of *A. fumigatus* bind to the cell surface and penetrate the cell with 30% efficiency, although most of the endocytosed conidia do not germinate [10]. The presence of conidia causes injury, seen as rounding and detachment from surfaces, to A549 cells. However, the morphological integrity of

Received 9 September 2003; accepted 11 December 2003; electronically published 11 May 2004.

Financial support: Israel Academy of Sciences (grant 741/01 to N.O.).

Reprints or correspondence: Dr. N. Osherov, Dept. of Human Microbiology, Sackler School of Medicine, Tel Aviv University, Tel Aviv 69978, Israel (nosherov@post.tau.ac.il).

The Journal of Infectious Diseases 2004;189:1965–73

© 2004 by the Infectious Diseases Society of America. All rights reserved.
0022-1899/2004/18911-0001\$15.00

the invaded pneumocytes is preserved, even after invasion by growing hyphae [11]. Early during infection, 10%–20% of the infected A549 cells undergo apoptosis, but the majority of the cells die later (24 h) by necrosis [12]. Moreover, it has been demonstrated that the addition of fungal culture filtrate (CF) is sufficient to cause cell death. The components responsible for this effect have not yet been identified [13].

An important step toward understanding the disease state in invasive aspergillosis is to fully elucidate the molecular mechanisms operating in lung alveolar cells during their initial colonization with *A. fumigatus*. The cytoskeleton constitutes the basis for the formation and maintenance of a functional physical barrier between the cell and its surroundings. To better understand the ability of *A. fumigatus* to breach the alveolar barrier before invading the lung tissue, we investigated the cytoskeletal alterations induced by infection in the alveolar A549 cell line, with a special emphasis on the actin cytoskeleton. We studied the morphological changes that occur in actin, tubulin, and intermediate filament cytoskeletal fibers in the presence of germinating conidia or CF. Focal contacts that mediate interaction of the actin cytoskeleton with the extracellular matrix [14] were also investigated during infection. The role of secreted *A. fumigatus* proteases was examined by use of protease inhibitors and protease-deficient mutants.

Our findings indicate that *A. fumigatus* secretes proteases that perturb the organization of the actin cytoskeleton and focal contact sites of A549 lung pneumocytes. We demonstrate that addition of antipain, a serine and cysteine protease inhibitor, blocks these effects, suggesting that combining protease inhibitors with current antifungal treatments may reduce damage to endothelial cells at the site of infection and improve survival.

MATERIALS AND METHODS

Growth of conidia. *A. fumigatus* strain AF293 was used throughout this study. AF293 was originally isolated at autopsy from a patient with invasive pulmonary aspergillosis (<http://www.aspergillus.man.ac.uk>). The *A. fumigatus* (AF) ALP-deficient strain and its isogenic parental strain G10 have been described elsewhere [7]. Fungi were grown on YAG solid medium (0.5% wt/vol yeast extract, 1% dextrose, and 1.5% agar), for 3 days at 37°C, until conidia were mature.

Calcofluor staining of conidia. *A. fumigatus* conidia (10^9 conidia/mL) were incubated in a solution of 1 mg/mL calcofluor (Sigma) in a darkened orbital shaker, for 1 h at 37°C at 150 rpm. Conidia were washed twice with PBS, to remove free calcofluor, and were resuspended in PBS, to a concentration of 10^8 conidia/mL. Calcofluor staining did not affect viability or germination of conidia.

Preparation of fungal CF. Conidia were collected in a 0.01% (vol/vol) Tween 80 (Sigma) solution, washed twice in PBS, and

resuspended in 100 mL of Dulbecco's modified Eagle medium (DMEM) containing 10% fetal calf serum (FCS; Biological Industries), at a concentration of 1×10^6 conidia/mL. Fungal cultures were grown in an orbital incubator, for 48 h at 37°C at 200 rpm. These conditions have been shown elsewhere to produce a toxic CF [12]. Growth medium containing CF was decanted after centrifugation at 2300 g and filter sterilized.

A549 cell growth. Human cancer cell line A549 (ATCC CLL 185), derived from a human lung carcinoma [15], was grown in DMEM containing 10% FCS and 1% penicillin-streptomycin (Biological Industries) in 10-cm tissue-culture plates (Corning). Cells were incubated at 37°C, in 6% CO₂ and in a humidified atmosphere, and were routinely subcultured by trypsinization every 3–4 days.

A549 cell transfection. A549 cells were grown in a 35-mm tissue-culture plate, seeded at $\sim 1\text{--}3 \times 10^5$ cells/well in 2 mL of DMEM. The cells were grown at 37°C in a CO₂ incubator until 50%–80% confluent. Two solutions were prepared: solution A contained 95 μ L of serum-free DMEM and 5 μ g of plasmid pEGFP (green fluorescent protein)–actin (Clontech), and solution B contained 90 μ L of serum-free DMEM and 10 μ L of lipofectamine (Invitrogen). These 2 solutions were combined, mixed, and left for 20 min at room temperature. The mixture was then added to the cells that were diluted in 800 μ L of serum-free DMEM. The cells were placed in a CO₂ incubator for 5 h. After incubation, the transfection mix was replaced with standard medium. The maximum level of expression of GFP (green fluorescent protein)–actin was observed within 48 h after transfection.

Vinculin and actin coimmunostaining. Cells were fixed for 30 min at room temperature in PBS containing 3% (vol/vol) paraformaldehyde and were permeabilized with 0.5% (wt/vol) Triton X-100 for 3 min. Subsequently, cells were incubated for 40 min at room temperature with a monoclonal antibody to vinculin, at a dilution of 1:100 (Sigma). Cells were then washed 3 times with PBS, after which rhodamine-phalloidin (for actin-staining) diluted 1:75 and Alexa 488 goat anti-mouse antibody (Molecular Probes) diluted 1:200 (for staining of the anti-vinculin antibodies) were added for 40 min at room temperature. Cells were then washed 3 times in PBS and viewed by use of microscopy.

Microtubule and cytokeratin 18 immunostaining. Cells were fixed in cold methanol (–20°C) for 20 min at –20°C, washed in PBS for 15 min, incubated in 0.5% Triton X-100 for 3 min, and washed again 3 times in PBS. A monoclonal antibody to tubulin (Sigma) or cytokeratin 18 (Research Diagnostics) was added for 40 min and washed as described above. Alexa 558 goat anti-mouse antibody (Molecular Probes) diluted 1:200 was then added to the cells for 40 min at room temperature, and the cells were washed 3 times in PBS and viewed by use of microscopy.

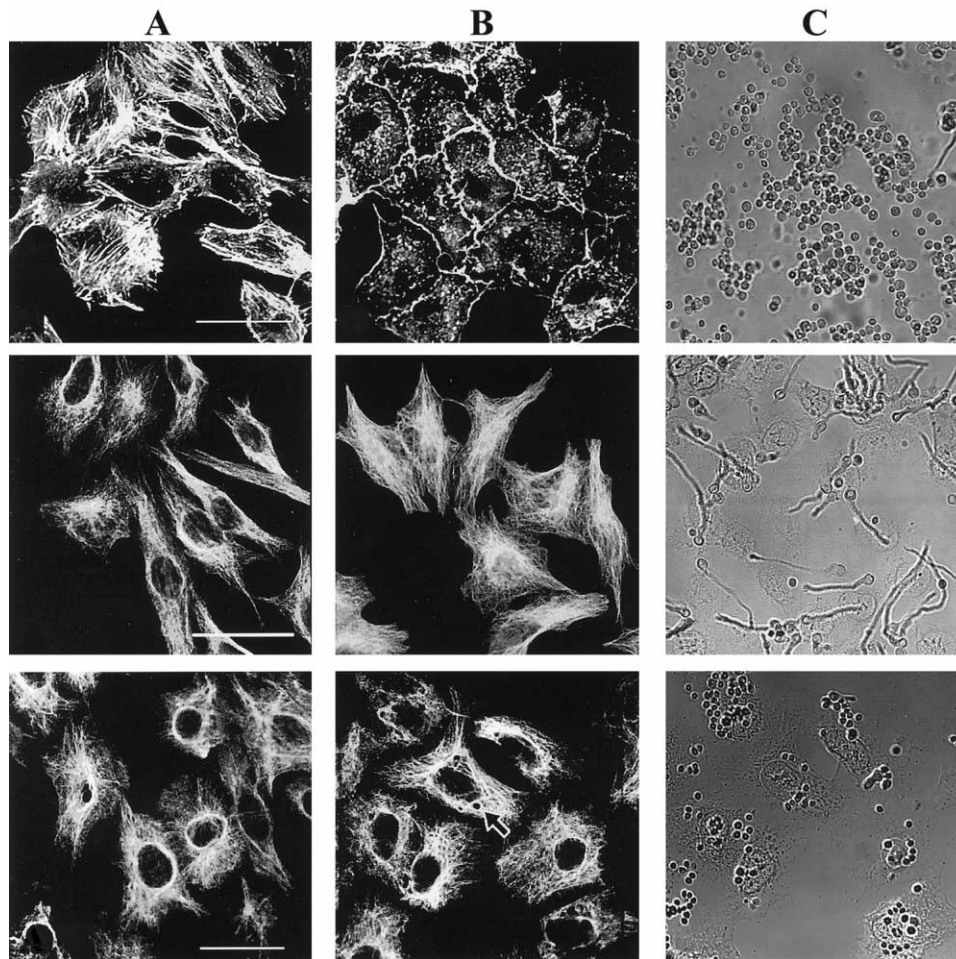


Figure 1. Immunostaining of *Aspergillus fumigatus*-infected A549 cells with actin (*top panels*), microtubule (*middle panels*), and intermediate-filament cytokeratin-18 (*lower panels*). *A*, Uninfected A549 cells. *B*, A549 cells after 8 h of incubation with conidia. *C*, Phase contrast of panel *B*. Bar, 20 μm (for all images).

Confocal laser scanning microscope (CLSM) analyses.

Analyses were performed by use of a Zeiss CLSM 410 equipped with a 25-mW krypton-argon laser and a 10-mW helium-neon laser (488 nm and 543 nm). Images were printed by use of a Codonics NP1600 printer.

Protease inhibitor studies. Protease inhibitors (all obtained from Sigma) were added to the CF at the following concentrations, as recommended by the manufacturer: the serine and cysteine protease inhibitor antipain (10 $\mu\text{g}/\text{mL}$; stock 0.5 mg/mL in H_2O), the aspartic protease inhibitor pepstatin (1 $\mu\text{mol}/\text{L}$; stock 1 mmol/L in 10% [vol/vol] acetic acid), the metalloprotease inhibitor galardin (13 $\mu\text{mol}/\text{L}$; stock 1 mmol/L in DMSO), the cysteine protease inhibitor E-64 (1 $\mu\text{mol}/\text{L}$; stock 0.1 mmol/L in H_2O), and the serine protease inhibitor aprotinin (2 $\mu\text{g}/\text{mL}$; stock 10 mg/mL in H_2O). General proteolytic activity was measured by use of the azocasein assay [15]. Azocasein (5 mg/mL; Sigma) was dissolved in 50 mmol/L Tris-HCl (pH 7.5), 0.2 mol/L NaCl, 5 mmol/L CaCl_2 , 0.05%

Triton X-100, and 0.01% (wt/vol) sodium azide. A 400- μL aliquot of this solution was mixed with 100 μL of CF in the presence or absence of specific protease inhibitors. After overnight incubation at 37°C, 150 μL of 20% (vol/vol) trichloroacetic acid was added. After 30 min at room temperature, the tubes were centrifuged at 16,000 g for 3 min, and the pellets were discarded. The supernatant was mixed with an equal volume of 1 mol/L NaOH, and absorption of the liberated dye was measured at 436 nm.

XTT (2,3-bis-[2-methoxy-4-nitro-5-sylfophenyl]-2H-tetrazolium-5-carboxanilide, disodium salt) cell viability assay. A549 cells were grown in 96-well cell-culture plates (Corning), to 80% confluency. CF was added to the cells in the presence or absence of protease inhibitors. After 24, 48, and 72 h of incubation, XTT reagent (Beit HaEmek) was added, and the colorimetric assay was performed as specified by the manufacturer. Absorbance (optical density at 490 nm) was read on an ELISA reader (Spectra MAX 340; Molecular Devices).

Cell adherence assay. A549 cells at 80% confluence were incubated in 6-well plates (Nalge Nunc), in the presence of CF and protease inhibitors. After 24, 48, and 72 h of incubation, the wells were washed 3 times with PBS, to remove nonadherent cells. The remaining cells were detached by trypsinization and counted on a hemocytometer.

Statistical analysis. The XTT viability and adherence experiments shown in figure 7 were independently performed 3 times. A representative experiment is displayed. Error bars denote SDs. *P* values were calculated by use of Student's *t* test. Differences were considered to be statistically significant if *P* < .05.

RESULTS

Perturbation of the actin cytoskeleton in A549 cells exposed to *A. fumigatus* conidia or fungal CF. Actin fiber, microtubule, and intermediate-filament fibers of infected A549 cells were stained with phalloidin–fluorescein isothiocyanate (FITC) (figure 1, *top*), antitubulin (figure 1, *middle*), and anti–cytokeratin 18 antibodies (figure 1, *bottom*), respectively. We observed the cells at various time points between 0.5 and 10 h of incubation in the presence of conidia or CF. Actin stress fibers were rapidly disrupted in infected cells, whereas, at all time points, the cells preserved their microtubule and intermediate filament structures without any noticeable changes. Of interest, both tubulin and cytokeratin filaments were excluded from the vicinity of the endocytosed conidia (figure 1B, *bottom*, arrow).

Disruption of actin fibers, membrane blebbing, and formation of actin aggregates in infected A549 cells. We performed time-course analysis of the actin cytoskeleton in A549 cells exposed to *A. fumigatus* conidia (figure 2, *right*) or CF (figure 2, *left*). In both cases, the changes in the actin cytoskeleton were remarkably similar. Untreated A549 cells in culture exhibit pronounced actin stress fibers and a concentrated actin “mesh” near the plasma membrane (figure 2, *top*). Thirty minutes after the addition of conidia, the number of cytoplasmic actin stress fibers decreased markedly, and membrane blebbing began. After 2 h, stress fibers were completely disrupted, whereas the peripheral actin mesh remained intact (figure 2, panels marked “2 h”). Approximately 30% of the cells had undergone membrane blebbing at this stage (figure 2, arrows in panels marked “2 h”). After 8 h, irregularly polymerized actin aggregates appeared in the cytoplasm (figure 2, panels marked “8 h”). These structures persisted throughout the 24-h experiment.

After 24 h of infection, most of the actin cytoskeleton was depolymerized, as seen by the lack of actin stress fibers and the starlike shape of the infected cells (figure 2, panels marked “24 h”). The peripheral actin mesh, which had preserved its shape during the previous stages, was also disrupted at this stage.

Induction of membrane blebbing. Infected A549 cells underwent pronounced membrane blebbing between 30 min and

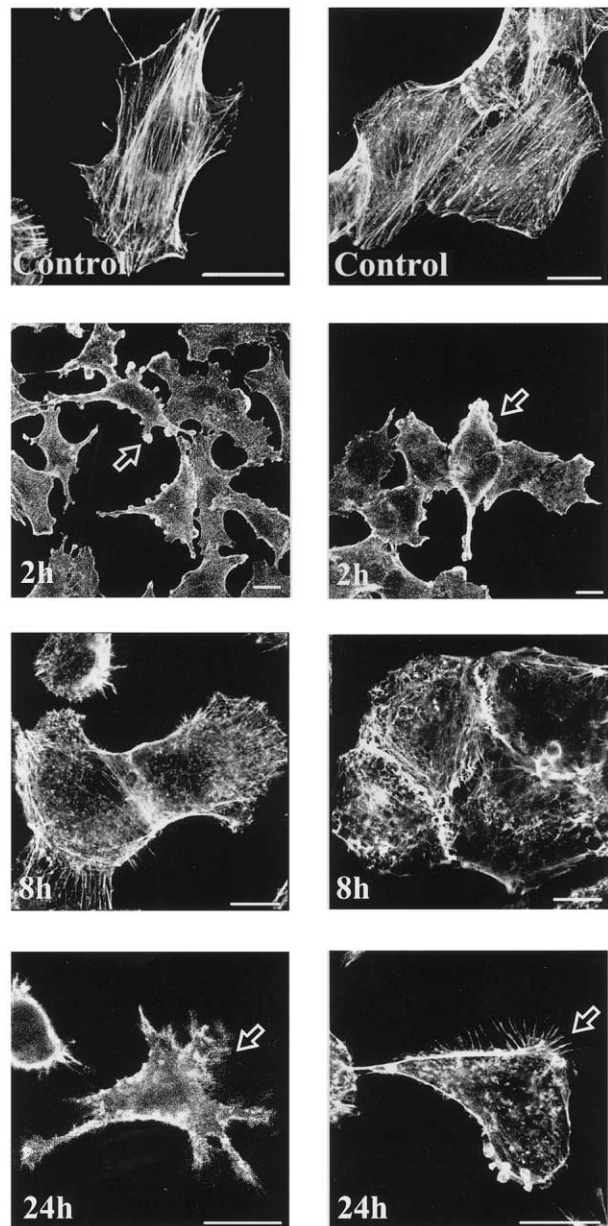


Figure 2. Reorganization of actin fibers and membrane blebbing in A549 cells infected with *Aspergillus fumigatus* conidia or culture filtrate (CF). Infected A549 cells were stained for actin with rhodamine-phalloidin. *Left*, changes in actin organization and membrane blebbing in the cells in the presence of CF; *right*, changes in actin organization and membrane blebbing in the cells in the presence of conidia. The arrows at 2 h highlight membrane blebbing.

2 h after the addition of *A. fumigatus* conidia or CF. A549 cells were stained with rhodamine-phalloidin at various time points after infection, and the number of cells undergoing membrane blebbing was counted. Between 30 min and 2 h after infection, the percentage of cells undergoing membrane blebbing was maximal (25%–29%) (figure 3, *top*). Membrane blebbing was decreased to 10% at 8 h. Infection with either conidia or CF demonstrated comparable kinetics.

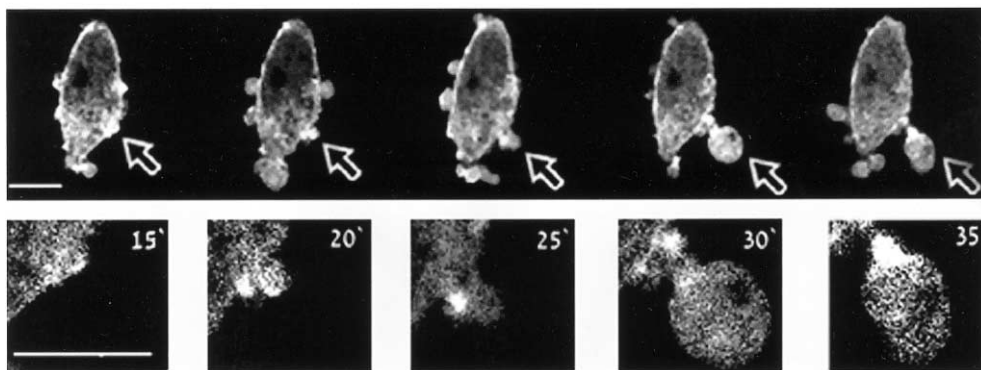
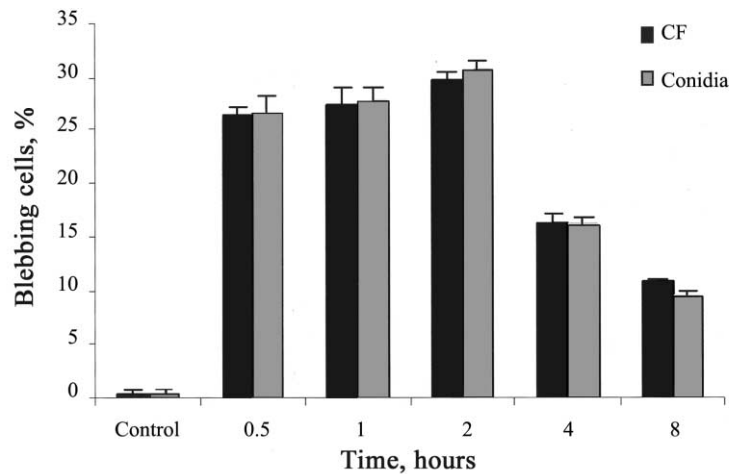


Figure 3. *Top*, Time course of conidial and culture filtrate–induced A549 cell membrane blebbing. For each time point, ~500 rhodamine-phalloidin–stained A549 cells were analyzed by use of fluorescence microscopy and were scored for blebbing. The results are representative of 3 independent experiments performed in triplicate and are expressed as the mean + SD (error bars) of 3 replicates. *Bottom*, Green fluorescent protein–actin–transfected A549 cells undergo rapid membrane blebbing within 1 h after addition of *Aspergillus fumigatus* conidia. Images were recorded at 5-min intervals. The arrow highlights a rapidly forming bleb. Bar, 10 μ m.

To analyze membrane blebbing in living A549 cells, we transfected them with GFP-actin and monitored the cells during infection with conidia. Approximately 30% of the cells underwent membrane blebbing. A representative set of images of a single living cell, taken 1 h after infection, demonstrates the occurrence of blebbing (figure 3, *bottom*).

Endocytosing of viable and heat-killed conidia into A549 cells and surrounding of conidia by an actin-rich ring structure. Confocal Z-sections (cross sections) of infected A549 cells produced with a CLSM demonstrated that, after 30 min of incubation, a proportion of the added conidia had attached to the cell surface (figure 4A). After 4 h, some of the attached conidia had undergone endocytosis (figure 4B). After 8 h of incubation, the internalized conidia were surrounded by pronounced actin-rich structures (called the “actin ring”) (figure 4C). Heat-killed conidia were endocytosed to the same extent as live conidia, including the formation of an actin ring around each spore (figure 4D). In contrast to the results obtained with

live conidia, no other actin rearrangements were observed, and actin stress fibers were preserved in the infected cells.

Disruption of focal contacts during infection. To visualize focal contacts in the infected cells, we labeled vinculin, a key component of these structures. Coimmunofluorescent staining of untreated A549 cells with anti-vinculin antibodies and phalloidin-FITC (actin-staining) showed numerous focal contacts on the edge of the cell, located at the ends of actin stress fibers (figure 5A, *arrow*). After 2 h of incubation with conidia, vinculin staining of focal contacts diminished markedly, indicating destruction of focal contacts in most cells (figure 5B and 5F). Destruction of focal contacts took place at the same time as disruption of actin stress fibers. Incubation of A549 cells with CF had the same effect on localization of vinculin as did incubation with conidia, suggesting that factors secreted by the fungus are responsible for these changes (figure 5C).

Involvement of secreted fungal serine and cysteine proteases in disrupting the actin cytoskeleton of infected A549 cells.

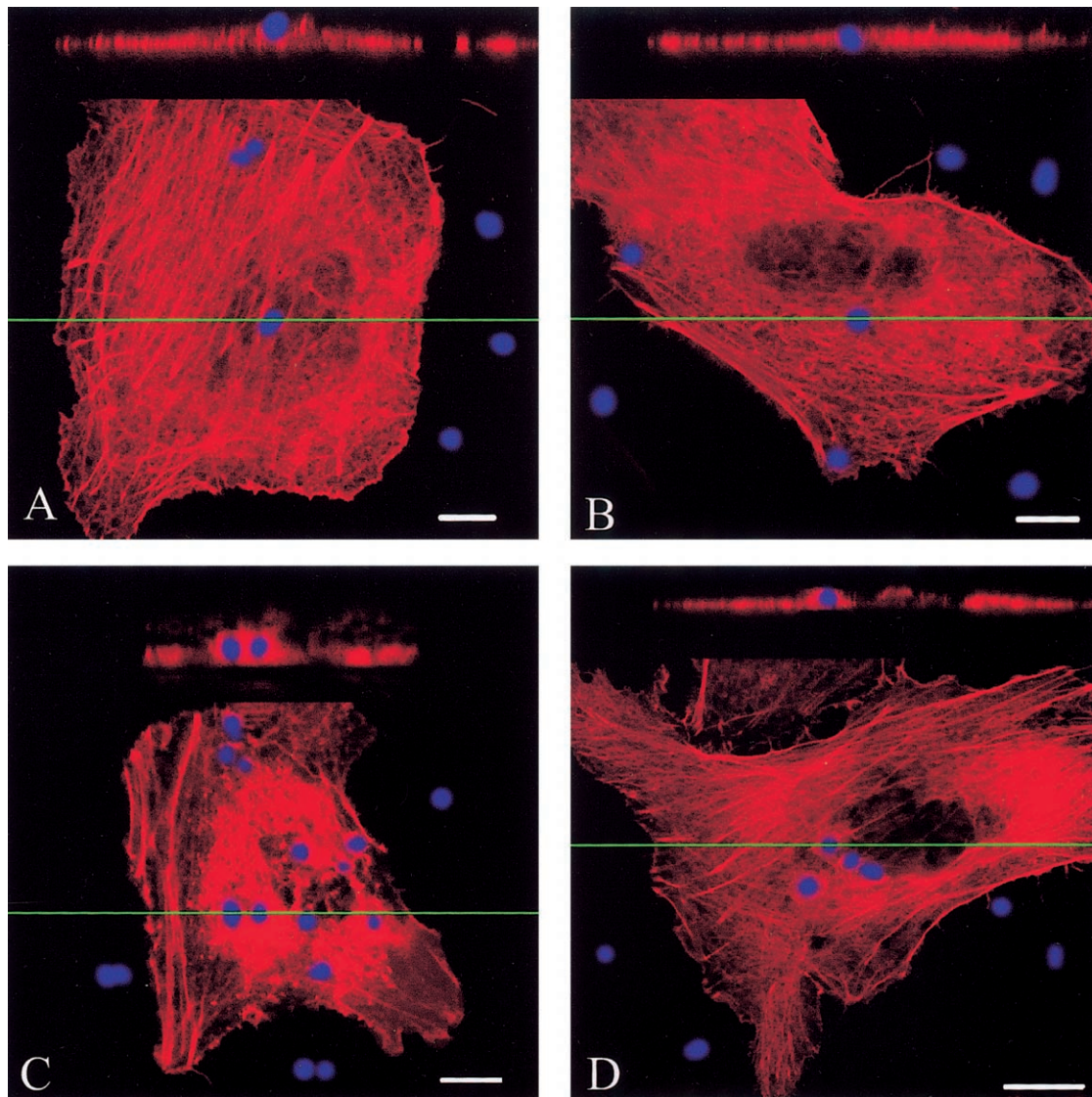


Figure 4. Interaction of A549 cells with *Aspergillus fumigatus* conidia. Conidial adhesion and penetration is revealed by Z-sections (cell cross-sections) shown above each overhead image. The location of the Z-section in the infected cell is highlighted by a thin green line traversing the cell (lower part of each image). Conidia attach to the cells after 30 min (A) and penetrate after 4 h of incubation (B). After 8 h, endocytosed conidia are encapsulated in actin ring structures (C). Heat-killed conidia are also endocytosed and surrounded by an actin ring after 8 h of incubation with A549 cells. Actin stress fibers are clearly seen, preserved in cells infected with heat-killed conidia (D). Bar, 10 μ m.

We hypothesized that the disruption of the actin cytoskeleton in infected A549 cells is a result of secreted fungal proteases. To test this hypothesis, A549 cells were incubated in the presence of CF and several different classes of protease inhibitors, including antipain, aprotinin, pepstatin, galardin, and E-64. Only antipain markedly reduced actin cytoskeleton disruption and focal adhesion site detachment in infected cells (figure 5D). To further support these findings, we took advantage of an *A. fumigatus* mutant strain in which the major secreted serine protease, *AF-ALP*, has been deleted. CF derived from this strain was substantially reduced in its ability to disrupt the actin cytoskeleton of infected cells (figure 5E). We directly measured

total protease activity in the different CFs by using azocasein as a protease-specific substrate. Antipain reduced wild-type (strain AF293) CF protease activity by ~67%. The protease activity of the *AF-ALP*-deficient strain was reduced by 70%, compared with its isogenic control, strain G10 (figure 6).

Delay of A549 cell death and detachment from the matrix caused by inhibition of CF protease activity. On the basis of the ability of antipain to block damage to the actin cytoskeleton of infected A549 cells, we reasoned that it might also delay later events, such as detachment and death of cells. Therefore, we incubated A549 cells in the presence of CF, with or without antipain, and CF derived from the *AF-ALP*-deficient

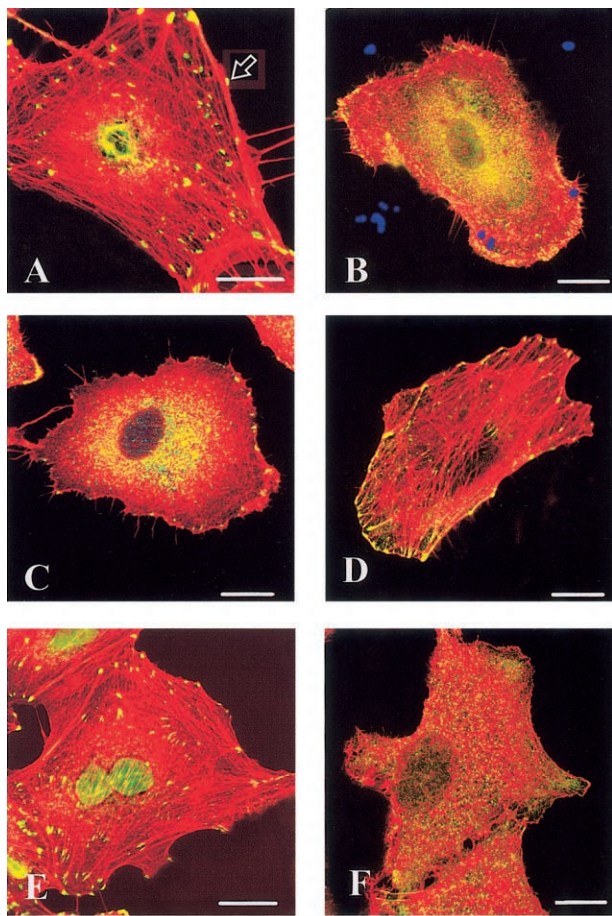


Figure 5. Actin and vinculin/focal adhesion disruption in infected A549 cells. Cells were coimmunostained for actin (red) and vinculin (green). A, Uninfected A549 cells. Focal adhesion sites (green dots) are highlighted by the arrow. A549 cells were infected for 8 h with *Aspergillus fumigatus* (strain AF293) calcofluor-stained conidia (B; blue), culture filtrate (C), filtrate and antipain (D), filtrate from an *A. fumigatus* ALP-deficient mutant (E), or filtrate from a control G10 strain (F). Note the extensive redistribution of actin and vinculin in infected cells. Bar, 15 μ m.

strain. Cell viability was measured by use of an XTT colorimetric assay, and adhesion was measured by counting adherent cells after repeated washes. Our results indicate that, when A549 cells are incubated with either wild-type *A. fumigatus* CF in the presence of antipain or CF prepared from the *AF-ALP*-deficient strain, the loss in A549 cell viability and adherence is significantly reduced, by ~50% after 24 h of incubation (figure 7). This protective effect decreased at later time points, suggesting that, in addition to proteases, other fungal-secreted factors are involved in these processes.

DISCUSSION

Fungal infections are responsible for significant morbidity and mortality in both animals and humans. Over the course of the

last 2 decades, there has been a substantial increase in the incidence of human fungal infections among immunocompromised individuals. *A. fumigatus* is a saprophytic fungus responsible for the most common mold infection worldwide. Inhalation of infectious conidia and their deposition in the alveoli can lead to germination and growth of the fungus in the lung and, in severely immunocompromised individuals, can develop into a potentially deadly infection known as invasive aspergillosis. Even with early diagnosis and aggressive antifungal treatment, mortality is >60%.

In the present study, we focused on the cytopathological effects of *A. fumigatus* on cultured alveolar type II-like cells during the early stages of infection (up to 24 h). We used A549 lung pneumocytes as an experimental model. This cell line displays the same metabolic and morphological characteristics as type II alveolar epithelial cells [16] and has been used extensively as a model system for studying *Aspergillus* infection [10–13]. During observation of the samples, we concentrated on the following events: general alterations in shape; changes in distribution of cellular actin, focal contact, microtubule, and intermediate filament; and characteristic features of contact sites between conidia and cells.

We have shown that, during the first 2 h of infection, ~30% of the infected A549 cells undergo membrane blebbing. Membrane blebbing has been shown to take place in response to stress factors (e.g., oxidative stress and cold shock) and during the early stages of the apoptotic response. Blebbing also occurs in DLPK (squamous lung carcinoma) cells exposed to *A. fumigatus* CFs, but this did not lead to the formation of apoptotic bodies, and the cells died after loss of membrane integrity, indicating necrosis [12].

Strikingly, we have demonstrated that, of the 3 major classes of cytoskeletal fibers—actin microfilaments, microtubules, and intermediate filaments—only the actin cytoskeleton undergoes

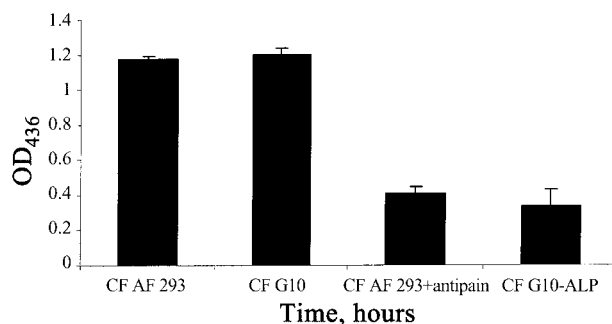


Figure 6. Inhibition, by antipain, of culture filtrate (CF) protease activity in *Aspergillus fumigatus* wild-type strains AF293 and G10. The *A. fumigatus* ALP-deficient strain shows reduced CF protease activity. Protease activity was determined by use of the azocasein assay, as described in Materials and Methods. The results are representative of 3 independent experiments performed in triplicate and are expressed as the mean + SD (error bars) of 3 replicates.

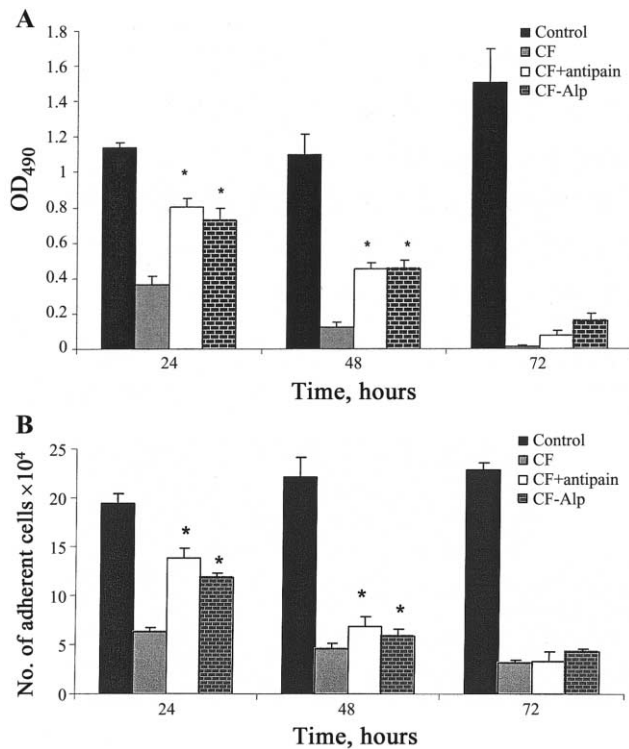


Figure 7. A, Culture filtrate (CF)-induced loss of A549 cell viability, as measured by XTT (2,3-bis-[2-methoxy-4-nitro-5-sylfophenyl]-2H-tetrazolium-5-carboxanilide, disodium salt) assay. B, Reduction of adhesion by antipain in the *Aspergillus fumigatus* ALP-deficient strain. The XTT and cell-adhesion assays are described in Materials and Methods. The results are representative of 3 independent experiments performed in triplicate and are expressed as the mean + SD (error bars) of 3 replicates. * $P < .05$, vs. untreated A549 cells in the presence of wild-type CF.

major structural changes in response to infection. Actin stress fibers disappear and are replaced by actin aggregates. Destruction of actin stress fibers has been demonstrated in cultured cell lines in response to infection with *Candida albicans* and *Salmonella enterica* [17–20] and may be a general response to infection. Actin fiber clumping and formation of actin aggregates take place in cells after various physical and chemical insults (e.g., ischemia and energy depletion, UV irradiation, and treatment with calcium ionophores) [21] and are indicative of disorganization and fragmentation of actin fibers. Of importance, we have also observed similar disruptive effects on the actin cytoskeleton in *A. fumigatus*-infected NIH 3T3 fibroblasts, Hep2 epithelial cells, and human foreskin fibroblasts by using conidia from *A. fumigatus*, *Aspergillus niger*, *Aspergillus terreus*, and *Aspergillus flavus* (authors' unpublished data). These results suggest that a common underlying mechanism is involved in these changes and that the fungus may activate these changes wherever it causes infection, irrespective of cell and tissue type.

Loss of focal contacts was also noted in infected A549 cells.

Because focal contacts anchor the cell to the substrate, this process may enable growing hyphae to penetrate between and beneath attached cells and may play a role during invasion of tissues.

Previous works have noted that the internalization of conidia depends on the ability of the infected cells to polymerize actin [10]. In the present report, we have demonstrated that both live and heat-killed conidia are endocytosed in actin-coated vesicles and surrounded by an actin ring. This result suggests that the cellular actin cytoskeleton interacts with preexisting, heat-stable, cell-wall conidial components. Of note, heat-killed conidia do not induce actin-cytoskeleton rearrangements, indicating that these changes necessitate active metabolism and functional biosynthetic pathways.

The dramatic effects on membrane blebbing and disruption of actin fibers and focal contact are probably induced by factors secreted by the fungus, because they all occur when CF alone is added to the cells. Several lines of evidence suggest that secreted fungal proteases are responsible for the loss of actin fibers and focal contacts in infected A549 cells: we have demonstrated that antipain blocks this process and that CF from an *AF-ALP*-deficient strain fails to induce damage to the actin cytoskeleton after 8 h, despite the fact that they retained ~30% of azocasein protease activity. A single serine protease, *AF-ALP*, has been cloned and characterized in *A. fumigatus*, although a search that we conducted in the *A. fumigatus* genome TIGR database (available at: <http://www.tigr.org/tdb/>) revealed at least 2 additional sequences predicted to encode serine proteases. At present, no cysteine proteases have been identified in *A. fumigatus*, although the *A. fumigatus* TIGR genome database contains a single cysteine protease with homology to *Aspergillus nidulans* PalB, a calpain-like, calcium-activated cysteine protease. It is worth noting that antipain was most effective at blocking the effects measured on the infected cells, whereas selective serine (aprotinin) and cysteine (E-64) inhibitors were only partially effective. In contrast, the damaging activity of CF derived from the *ALP*-deficient strain, which presumably still contains cysteine protease activity, was similar to that of the antipain-treated wild-type CF. This apparent discrepancy may simply reflect the variable and imprecise selectivity of the different protease inhibitors, or it may suggest that, in the *ALP*-deficient strain, loss of serine protease activity also leads to a reduction in cysteine protease activity. Alternatively, the antipain-treated and *ALP*-deficient strains may compensate by up-regulating metalloproteases; this compensatory protease secretion was observed in a serine protease-deficient mutant of *A. flavus* [22].

The contribution of proteases secreted by *A. fumigatus* to its pathogenicity remains unclear. Kauffman et al. [23] have shown that *A. fumigatus* CFs induce cytokine release, cell shrinkage, and desquamation in A549 cells and that this release is blocked

by the addition of serine and cysteine protease inhibitors. Ikegami et al. [24] have demonstrated that CF derived from an *AF-ALP*-deficient-strain is deficient in its ability to inhibit polymorphonuclear leukocyte chemotaxis. In the present report, we have demonstrated a link between protease activity and damage to the actin cytoskeleton, focal adhesion, cell adhesion, and viability. There are several mechanisms that may explain how proteases mediate these effects. The first possible mechanism is external action through specific cellular signal-transduction pathways (e.g., the integrin receptor/focal contact-signaling pathways), perhaps by proteolytic cleavage of the receptor, or through activation of the receptor by cleaved components of the extracellular matrix. Of interest, Karragher et al. [25] have shown that protease-degraded collagen fragments promote rapid disassembly of smooth-muscle focal adhesions that correlate with cleavage of pp125^{FAK} paxillin and talin. The second possible mechanism is internal action that follows endocytosis of fungal-secreted proteases. Indeed, it has been demonstrated that caspase 3-induced proteolytic cleavage of focal adhesion kinase (pp125^{FAK}), an important component of the focal adhesion complex, results in disassembly of focal contacts, cell rounding, and apoptosis [26].

Future research should focus on isolating and identifying the cellular components that interact with the fungal-secreted proteases and on delineating the cellular signaling pathways through which they act. In addition, the results of our present study suggest that combining protease inhibitors with current antifungal treatments may reduce damage to endothelial cells at the site of infection.

Acknowledgments

We thank Sophie Paris and Jean-Paul Latge, for providing us with the *ALP*-deficient and G10 *Aspergillus fumigatus* strains; Itamar Shalit and all members of the laboratory or Nir Osherov, for critical reading of this manuscript; and Benny Geiger, for valuable discussion and suggestions.

References

- Latge JP. *Aspergillus fumigatus* and aspergillosis. *Clin Microbiol Rev* **1999**; *12*:310–50.
- Bouchara JP, Sanchez M, Esnault K, Tronchin G. Interactions between *Aspergillus fumigatus* and host matrix protein. *Contrib Microbiol* **1999**; *2*:167–81.
- Wasylnka JA, Moore MM. Adhesion of *Aspergillus* species to extracellular matrix proteins: evidence for involvement of negatively charged carbohydrates on the conidial surface. *Infect Immun* **2000**; *68*:3377–84.
- Moutaouakil M, Monod M, Prevost MC, Bouchara JP, Paris S, Latge JP. Identification of the 33-kDa alkaline protease of *Aspergillus fumigatus* in vitro and in vivo. *J Med Microbiol* **1993**; *39*:393–9.
- Kunert J, Kopecek P. Multiple forms of the serine proteinase *ALP* of *Aspergillus fumigatus*. *Mycoses* **2000**; *43*:339–47.
- Monod M, Paris S, Sanglard D, Jatton-Ogay K, Bille J, Latge JP. Isolation and characterization of a secreted metalloprotease of *Aspergillus fumigatus*. *Infect Immun* **1993**; *61*:4099–104.
- Monod M, Paris S, Sarfati J, Jatton-Ogay K, Ave P, Latge JP. Virulence of alkaline protease-deficient mutants of *Aspergillus fumigatus*. *FEMS Microbiol Lett* **1993**; *106*:39–46.
- Reichard U, Eiffert H, Ruchel R. Purification and characterization of an extracellular aspartic proteinase of *Aspergillus fumigatus*. *J Med Vet Mycol* **1994**; *32*:427–36.
- Latge JP. The pathobiology of *Aspergillus fumigatus*. *Trends Microbiol* **2001**; *9*:382–9.
- Wasylnka JA, Moore MM. Uptake of *Aspergillus fumigatus* conidia by phagocytic and nonphagocytic cells in vitro: quantitation using strains expressing green fluorescent protein. *Infect Immun* **2002**; *70*:3156–63.
- DeHart DJ, Agwu DE, Julian NC, Washburn RG. Binding and germination of *Aspergillus fumigatus* conidia on cultured A549 pneumocytes. *J Infect Dis* **1997**; *175*:146–50.
- Daly P, Verhaegen S, Clynes M, Kavanagh K. Culture filtrates of *Aspergillus fumigatus* induce different modes of cell death in human cancer cell lines. *Mycopathologia* **1999**; *146*:67–74.
- Daly P, Kavanagh K. Immobilization of *Aspergillus fumigatus* colonies in a soft agar matrix allows visualization of A549 cell detachment and death. *Med Mycol* **2002**; *40*:27–33.
- Zamir E, Geiger B. Molecular complexity and dynamics of cell-matrix adhesions. *J Cell Sci* **2001**; *114*:3583–90.
- Gifford AHT, Klippenstein JR, Moore MM. Serum stimulates growth of and proteinase secretion by *Aspergillus fumigatus*. *Infect Immun* **2002**; *70*:19–26.
- Foster KA, Oster CG, Mayer MM, Avery ML, Audus KL. Characterization of the A549 cell line as a type II pulmonary epithelial cell model for drug metabolism. *Exp Cell Res* **1998**; *243*:359–66.
- Tsarfaty I, Sandovsky-Losica H, Mittelman L, Berdicevsky I, Segal E. Cellular actin is affected by interaction with *Candida albicans*. *FEMS Microbiol Lett* **2000**; *189*:225–32.
- Drams S, Cossart P. Intracellular pathogens and the actin cytoskeleton. *Annu Rev Cell Dev Biol* **1998**; *14*:137–66.
- Filler SG, Swerdloff JN, Hobbs C, Luckett PM. Penetration and damage of endothelial cells by *Candida albicans*. *Infect Immun* **1995**; *63*:976–83.
- Finlay BB, Ruschkowski S, Dedhar S. Cytoskeletal rearrangements accompanying *Salmonella* entry into epithelial cells. *J Cell Sci* **1991**; *99*:283–96.
- Kuhne W, Besselmann M, Noll T, Muhs A, Watanabe H, Piper HM. Disintegration of cytoskeletal structure of actin filaments in energy-depleted endothelial cells. *Am J Physiol* **1993**; *264*:H1599–608.
- Ramesh MV, Kolattukudy PE. Disruption of the serine proteinase gene (*sep*) in *Aspergillus flavus* leads to a compensatory increase in the expression of a metalloproteinase gene (*mep20*). *J Bacteriol* **1996**; *178*:3899–907.
- Kauffman HF, Tomee JF, van de Riet MA, Timmerman AJ, Borger P. Protease-dependent activation of epithelial cells by fungal allergens leads to morphologic changes and cytokine production. *J Allergy Clin Immunol* **2000**; *105*:1185–93.
- Ikegami Y, Amitani R, Murayama T, et al. Effects of alkaline protease or restrictocin deficient mutants of *Aspergillus fumigatus* on human polymorphonuclear leukocytes. *Eur Respir J* **1998**; *12*:607–11.
- Carragher NO, Levkau B, Ross R, Raines EW. Degraded collagen fragments promote rapid disassembly of smooth muscle focal adhesions that correlates with cleavage of pp125(FAK), paxillin, and talin. *J Cell Biol* **1999**; *147*:619–30.
- Levkau B, Herren B, Koyama H, Ross R, Raines EW. Caspase-mediated cleavage of focal adhesion kinase pp125FAK and disassembly of focal adhesions in human endothelial cell apoptosis. *J Exp Med* **1998**; *187*:579–86.